Available online at www.sciencedirect.com
ScienceDirect
Dyes and Pigments 76 (2008) 447–454
DYES and PIGMENTS
www.elsevier.com/locate/dyepig

Synthesis and structure of α-azo-2-ketomethylquinolines

H. Loghmani-Khouzani*, H. Sabzyan, A. Rezaei-Pooranari

Department of Chemistry, University of Isfahan, Isfahan 81746-73441, Islamic Republic of Iran

Received 12 June 2006; accepted 2 October 2006
Available online 28 November 2006

Abstract

Sixteen α-phenylazo compounds derived from 2-ketomethylquinolines and two of their *N*-methyl derivatives were prepared. The structure of these compounds were studied using IR, UV, Mass, ^{1}H NMR and ^{13}C NMR spectroscopies, which revealed that all of the compounds exist exclusively in their azo form (**A**). Quantum mechanical PM3 computations were also carried out on the tautomers of two representative compounds to explain their relative stabilities and structures.

Keywords: Tautomerism; 2-Ketomethylquinolines; Enaminone; Hydrogen bonding; Azo–hydrazone; ^{1}H NMR and ^{13}C NMR; PM3

1. Introduction

2-Ketomethylquinolines contain the −N−C═C−C═O system in their structures and are classified as enaminones [1]. There have been a few reports on the nucleophilic reaction of 2-ketomethylquinolines; α-methylation and benzylation of 2-ketomethylquinolines with iodomethane and benzyl bromide in the presence of sodium hydride have been reported [2–5] in which it was mentioned that the dominant enaminone tautomer can be converted to the ketone tautomer via these reactions. The reaction of 2-ketomethylquinoline with bromine in chloroform [6,7] and in glacial acetic acid in the presence of anhydrous potassium acetate [4] has also been reported. Furthermore, the tautomerism of 2-ketomethylquinolines, including keto–enaminone equilibria, has been proven by different spectroscopic methods [3,4,8–11]. From previous studies of tautomerism in diazo compounds, it was shown that for compound **1**, the azo form **1-a** is in equilibrium with the hydrazone form **1-b** [12] while compound **2** is only in its hydrazone form [13] (Scheme 1).

A literature survey showed only one paper concerning an azo substituent at the α-position of 2-ketomethylquinolines (Compound **3j**, Scheme 1) [7], in which it was suggested that the compound is in the hydrazone form, without proposing any clear evidence. In order to have a fixed enaminone system, it is reported that the *N*-methyl derivatives of 2-ketomethylquinolines were prepared using methylketone and *N*-alkylquinolinium iodide in 10 N sodium hydroxide solution [14]. Azo colorants containing a hydroxyl and amino or conjugated carbonyl substituent group can, in principle, exist as mixtures of azo and hydrazone tautomers. Whilst azo–hydrazone tautomerism is quite interesting from a theoretical viewpoint, it is also important from practical standpoints, because the two tautomers have different properties [15].

Cheon et al. [12] studied azo–hydrazone tautomerism and hydrogen bonding in different compounds. These authors proposed that for a model arylazonaphthol, the equilibrium between the azo and hydrazone tautomers is rapidly established (within 0.2 ms on an NMR time scale) which renders ^{1}H NMR unsuitable for establishing the position of the tautomeric equilibrium. ^{15}N NMR, ^{14}N NMR and ^{13}C NMR methods have been employed to study the tautomeric equilibrium quantitatively [16–18]; these techniques showed that the model arylazonaphthol exists as a mixture of the azo and hydrazone forms.

This paper concerns the effects of diazo substitutents at the α-position of 2-ketomethylquinoline derivatives on tautomeric equilibria; both experimental and theoretical studies have

* Corresponding author. Tel.: +98 311 793 2722; fax: +98 311 6689732.
E-mail addresses: h.log119@sci.ui.ac.ir, loghmani_h@yahoo.com (H. Loghmani-Khouzani).

0143-7208/$ - see front matter © 2006 Elsevier Ltd. All rights reserved.
doi:10.1016/j.dyepig.2006.10.003

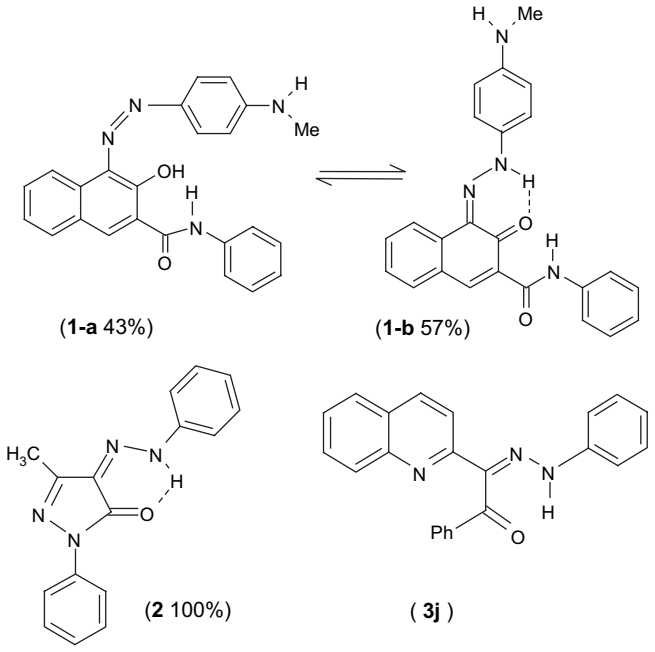

Scheme 1.

been carried out to shed some light on these tautomeric equilibria.

2. Experimental/Materials and methods

Chemicals were purchased from Aldrich, and were used without further purification. Diethylether was distilled above $CaCl_2$/Na before use. TLC was carried out using aluminium plates pre-coated with 0.2 mm silica gel (Kieselgel 60 F256) obtained from Merck; UV light was employed for visualization. Silica gel (Flash Kiesegel 60) was used for column chromatography. ^{1}H NMR and ^{13}C NMR spectra were obtained using deuterated solvents as internal standards; 300 MHz and 500 MHz spectra were recorded on a Bruker Avance BVT-3200 and AMX 500 MHz and Bruker Avance DRX 500 MHz spectrometers. Mass spectra were obtained using a Kratos MS80 RF spectrometer. Infrared spectra were recorded using a Nicolet 20-PC FTIR spectrometer; UV–vis spectra were recorded on a Shimadzu 160 spectrometer. All starting materials (2-ketomethylquinolines, R = Me, Et, *n*-Pr, Ph; Scheme 2) were prepared according to standard methods [3]. They were purified by passing through silica columns followed, for solids, by recrystallization to the corresponding constant melting points.

The general procedures used for the preparation of α-azo-2-ketomethylquinolines are as follows. At 0–5 °C, solutions of the corresponding benzene diazonium salts (1.0 mmol in 5 mL ethanol) were added dropwise to the solution of 2-ketomethylquinoline (1.0 mmol in 10 mL ethanol). The reaction mixture was refluxed and stirred under an argon atmosphere for 15 min. The resulting crude products were purified by flash chromatography using 20/80 ethylacetate/normal hexane solution as eluant. The pure products were obtained in 80–85% yields.

The synthesized compounds and their tautomeric structures and equilibria are introduced in Scheme 3 and Table 1.

3. Results and discussion

The α-azo-2-ketomethylquinolines synthesized and characterized in this research (Scheme 3 and Table 1) were studied using ^{1}H NMR, ^{13}C NMR, IR and UV spectroscopies; the most important features of the obtained spectra are summarized in Tables 2 and 3. The products contained both imino and azo groups in their structures, and therefore, several tautomeric forms, as shown in Scheme 3, can be predicted. It has been reported [10] that the ^{1}H NMR spectrum of the fixed enaminone shows two distinct doublets in the range 6–8 ppm due to C_3–H and C_4–H protons (for numbering of atoms see Scheme 2) which is a good method of distinguishing between compounds having aromatic quinoline ring and the fixed enaminone systems.

In the compounds under investigation, these distinct doublets appear in the range of 6–8 ppm, hence, structures **C**, **D**, **E** and **F** which are not considered as fixed enaminones

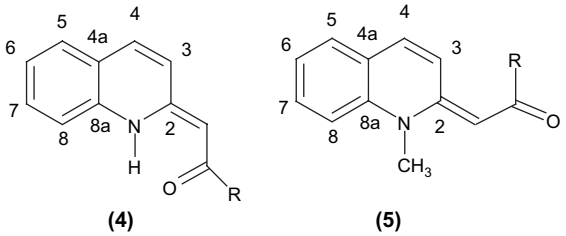

Scheme 2.

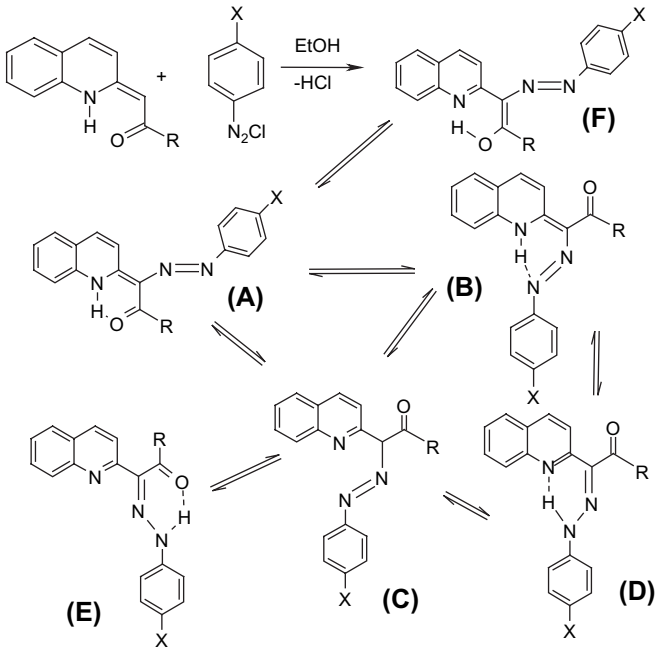

Scheme 3.

Table 1
α-Azo-2-ketomethylquinolines synthesized and studied in this work

Entry	R	X
3a	CH_3	H
3b	CH_2CH_3	H
3c	$CH_2CH_2CH_3$	H
3d	CH_3	Cl
3e	CH_2CH_3	Cl
3f	$CH_2CH_2CH_3$	Cl
3g	CH_3	NO_2
3h	CH_2CH_3	NO_2
3i	$CH_2CH_2CH_3$	NO_2
3j	C_6H_5	H
3k	C_6H_5	CH_3
3l	C_6H_5	Cl
3m	CH_2CH_3	CH_3
3n	C_6H_5	NO_2
3o	CH_3	CH_3
3p	$CH_2CH_2CH_3$	CH_3

due to the lack of the quinoline N–H group, are rejected. ^{1}H NMR spectra of the azo products do not show any peak for the methine C–H bond, but the enaminone N–H peak appears in the limited range 15.8–16.2 ppm (Table 2). The lower and upper limits of this range belong to **3c** and **3n**, respectively. These results show that electron-withdrawing group, *para*-nitro, in the X position, resulted in the deshielding of the enaminone proton. The electron-donating groups (R) in the α-position increased shielding of the enaminone proton; similarly, the range of chemical shifts obtained for the carbonyl ^{13}C of the compounds is very limited, i.e. between 191.37 and 201.22 ppm.

These two sets of data support the conclusion drawn already that only one tautomeric form (as the enaminone) exists dominantly for compounds **3a–p**. Furthermore, no strong carbonyl band in the IR spectra was observed around 1720 cm^{-1}; the carbonyl band for all of these compounds is located around 1660–1680 cm^{-1} due to the enaminone system (Table 3). It can therefore be concluded that structure **C** is not present in the equilibrium due to having a non-conjugated carbonyl system. Due to the interference with the water O–H band (3200–3400 cm^{-1}), it was not possible to assign and follow the enaminone N–H band in the IR spectrum. Furthermore, since the broad band around 3500 cm^{-1} appears identically for both **3c** and **6c**, it cannot be assigned to the N–H bond of the enaminone forms.

The ^{1}H NMR chemical shifts of the C_3–H and C_4–H protons for the model compound of the 2-ketomethylquinoline **4** with R = –COOEt in the α-position were found to be 7.96 and 8.14 ppm (with $J = 9.5$ Hz), respectively [4]. The UV spectrum of this compound shows absorption bands at 395, 285 and 218 nm in ethanol solution [19] which is comparable to that obtained for compounds **3a** and **3b** (Table 3). In these compounds, the ^{1}H NMR peaks of the C_3–H and C_4–H protons appear at 8.12 and 8.40 ppm (with $J = 8.96$ Hz), respectively. The difference between these data and those of the model compound of Ref. [4] is due to the lower electron-withdrawing effect of the azo-phenyl substituent in the α-position compared to that of the ethylester group.

The *N*-methyl derivatives **6c** and **6m**, (named so to show the correspondence with **3c** and **3m** compounds) shown in Scheme 4 and Tables 2 and 3, were synthesized. The IR spectra of the products **6c** and **6m** (Table 3 and Fig. 1) do not show any changes in the position of the carbonyl band compared to that of the *N*-methylated derivatives of 2-ketomethylquinoline **5** (introduced in Scheme 2, with R = *n*-Pr and Et) as references [3]. Furthermore, a comparison of the results reported in Tables 2 and 3 shows that the carbonyl bands in compounds **3a–p** appear at the same frequencies as observed for the corresponding *N*-methylated derivatives, **6c** and **6m**. It is thus expected that the compounds **3** are in their enaminone tautomeric forms **A** and **B**. Because of the lack of hydrogen bonding and steric hindrance of the *N*-methyl substitute, tautomers **A** and **B** are not well-defined distinct forms for compounds **6c** and **6m**, and thus only one conformational structure or an average conformational structure is possible for these compounds. Hence, a more direct comparison between the corresponding tautomers of compounds **6** and **3** is not possible. Cheon et al. [12] have reported that the UV absorption band for the diazo form **1a** appears around 500 nm but for the hydrazone form **1b** it appears at 570 nm. Since we did not observe any absorption band above 415 nm in the UV spectra of **3a–3p**, all of these compounds should be in one of their tautomeric forms only. Note the small variations of UV wavelengths reported in Table 3 which is much smaller than the differences between the two UV bands of **1-a** and **1-b**.

More information, especially X-ray crystallography and ^{15}N NMR, are necessary for the elucidation of the structures of the final products to distinguish between tautomeric structures **A** and **B** for these compounds.

4. Theoretical and computational studies

Semiempirical PM3 quantum mechanical computations [20] were carried out to characterize theoretically, on a comparative basis, the structures and stabilities of all tautomeric forms of the α-azo-2-ketomethylquinolines with $R = CH_3$ and X = H and NO_2 (compounds **3a** and **3g** in Table 1) as representatives. Analysis of the results of these computations are based on several structural and electronic properties such as intra-molecular hydrogen bond (HB), total binding energy, HOMO–LUMO gap (HLG), electric dipole moments and atomic charges, extension of the conjugation system, and aromaticity. The HyperChem program [21] was used in this computational study.

Analysis of the total binding energies calculated for the tautomers of these two representative compounds shows the following comparative orders for the thermochemical stabilities.

$$\text{Stability}: \begin{array}{ll} \mathbf{F} > \mathbf{A} > \mathbf{D} > \mathbf{B} > \mathbf{E} > \mathbf{C} > \mathbf{G} & (\mathbf{3a}: R = CH_3, X = H) \\ \mathbf{E} > \mathbf{A} > \mathbf{D} > \mathbf{F} > \mathbf{B} > \mathbf{C} > \mathbf{G} & (\mathbf{3g}: R = CH_3, X = NO_2) \end{array}$$

For both compounds **3a** and **3g**, the lack of HB considerably reduced the thermodynamic stability of the **G** tautomer compared to its two close relatives, **E** and **F**. This tautomer is the conformational isomer of the enol tautomers **E** or **F** in

Table 2
^{1}H NMR (300 MHz) and ^{13}C NMR (75 MHz) (both in ppm, referenced to TMS) data obtained in $CDCl_3$ for compounds **3a–p**, **6c** and **6m** introduced in Schemes 3 and 4, and Table 1

Entry	Chemical shift data
3a	^{1}H NMR: 2.71 (3H, s, CH_3), 7.00–7.96 (9H, m, C_9H_4N, C_6H_5), 8.12 (1H, d, $J = 8.96$ Hz, C_3–H), 8.41 (1H, d, $J = 8.96$ Hz, C_4–H), 15.85 (1H, s, NH) ^{13}C NMR: 27.31 (CH_3), 115.56, 123.17, 124.06, 127.30, 127.47, 128.47, 129.91, 130.19, 133.12, 136.70, 143.35, 145.71, 153.22 (aryl-C), 198.83 (C=O)
3b	^{1}H NMR: 1.30 (2H, q, CH_2), 3.21 (3H, t, CH_3), 7.10–7.98 (9H, m, C_9H_4N, C_6H_5), 8.13 (1H, d, $J = 8.96$ Hz, C_3–H), 8.40 (1H, d, $J = 8.96$ Hz, C_4–H), 15.85 (1H, s, NH) ^{13}C NMR: 27.31 (CH_3), 31.55 (CH_2), 115.08, 122.69, 123.51, 126.95, 127.05, 127.54, 128.08, 129.80, 136.25, 143.06, 145.36, 152.95 (aryl-C), 201.22 (C=O)
3c	^{1}H NMR: 1.00 (3H, t, CH_3), 1.80 (2H, m, CH_2), 3.11 (2H, t, CH_2), 7.10–8.70 (11H, m, C_9H_6N, C_6H_5), 15.80 (1H, s, NH) ^{13}C NMR: 14.19 (CH_3), 18.87 (CH_2), 40.01 (CH_2), 115.08, 122.77, 123.51, 127.07, 127.55, 128.08, 129.53, 129.81, 136.26 (aryl-C), 200.59 (C=O)
3d	^{1}H NMR: 2.80 (3H, t, CH_3), 7.10–8.70 (10H, m, C_9H_6N, C_6H_4), 15.90 (1H, s, NH) ^{13}C NMR: 26.91 (CH_3), 116.19, 122.81, 127.24, 128.03, 129.55, 136.43 (aryl-C), 199.23 (C=O)
3e	^{1}H NMR: 1.20 (3H, t, CH_3), 3.00 (2H, q, CH_2), 7.10–8.50 (10H, m, C_9H_6N, C_6H_4), 15.83 (1H, s, NH) ^{13}C NMR: 9.11 (CH_3), 31.55 (CH_2), 116.11, 122.75, 127.03, 127.57, 128.03, 128.26, 129.53, 132.69, 136.37, 141.80, 145.28, 152.80 (aryl-C), 201.01 (C=O)
3f	^{1}H NMR: 0.95 (3H, t, CH_3), 1.70 (2H, m, CH_2), 3.00 (2H, q, CH_2), 7.30–8.41 (10H, m, C_9H_6N, C_6H_4), 15.81 (1H, s, NH) ^{13}C NMR: 14.17 (CH_3), 18.79 (CH_2), 40.35 (CH_2), 116.10, 122.80, 127.01, 127.21, 127.57, 128.04, 128.27, 129.55, 129.85, 132.95, 136.36, 141.85, 145.29, 152.80 (aryl-C), 200.07 (C=O)
3g	^{1}H NMR: 2.76 (3H, s, CH_3), 7.31–8.46 (10H, m, C_9H_6N, C_6H_4), 16.11 (1H, s, NH) ^{13}C NMR: 27.00 (CH_3), 114.40, 123.00, 126.00, 127.35, 127.85, 128.12, 130.30, 136.00, 136.90, 142.85, 145.30, 148.20, 151.85 (aryl-C), 198.24 (C=O)
3h	^{1}H NMR: 1.18 (3H, t, CH_3), 3.10 (2H, q, CH_2), 7.20–8.40 (10H, m, C_9H_6N, C_6H_4), 15.90 (1H, s, NH) ^{13}C NMR: N.A.[a]
3i	^{1}H NMR: 0.97 (3H, t, CH_3), 1.8 (2H, m, CH_2), 3.1 (2H, q, CH_2), 7.25–8.4 (10H, m, C_9H_6N, C_6H_4), 15.81 (1H, s, NH) ^{13}C NMR: 14.09 (CH_3), 18.45 (CH_2), 40.51 (CH_2), 114.23, 122.91, 124.80, 127.31, 127.70, 127.80, 128.14, 130.29, 135.71, 136.08, 142.85, 145.43, 148.31, 152.02 (aryl-C), 200.70 (C=O)
3j	^{1}H NMR: 7.09–8.32 (16H, m, C_9H_6N, C_6H_5, C_6H_5), 16.10 (1H, s, NH) ^{13}C NMR: 115.20, 123.35, 123.55, 127.00, 127.15, 128.04, 129.50, 129.85, 131.55, 132.55, 136.55, 139.45, 143.18, 145.50, 154.08 (aryl-C), 193.40 (C=O)
3k	^{1}H NMR: 2.25 (3H, s, *p*-CH_3), 7.1–8.4 (15H, m, C_9H_6N, C_6H_4, C_6H_5), 16.0 (1H, s, NH) ^{13}C NMR: 19.22 (*p*-CH_3), 113.55, 120.58, 125.27, 125.45, 126.50, 128.22, 128.40, 129.05, 129.80, 131.53, 134.60, 138.07, 139.11, 143.82, 152.18 (aryl-C), 191.37 (C=O)
3l	^{1}H NMR: 7.0–8.25 (14H, m, C_9H_6N, C_6H_4, C_6H_4), 16.00 (1H, s, NH) ^{13}C NMR: 116.18, 122.18, 126.33, 127.62, 128.12, 129.28, 130.05, 130.60, 131.80, 133.11, 136.51, 141.82, 145.44, 152.18 (aryl-C), 192.37 (C=O)
3m	^{1}H NMR: 1.25 (3H, t, CH_3), 3.05 (2H, q, CH_2), 2.30 (3H, s, *p*-CH_3), 7.10–8.50 (10H, m, C_9H_6N, C_6H_5), 15.87 (1H, s, NH) ^{13}C NMR: 9.34 (CH_3), 20.90 (CH_2), 31.53 (*p*-CH_3), 115.05, 122.61, 126.89, 127.51, 128.04, 129.71, 130.05, 133.23, 136.16, 140.83, 145.34, 153.12 (aryl-C), 201.18 (C=O)
3n	^{1}H NMR: 7.31–8.35 (15H, m, C_9H_6N, C_6H_4, C_6H_5), 16.20 (1H, s, NH) ^{13}C NMR: 114.25, 122.25, 125.80, 127.20, 127.70, 127.90, 128.00, 128.07, 130.55, 135.55, 136.20, 137.00, 138.02, 142.52, 145.50, 152.60 (aryl-C), 192.24 (C=O)
3o	^{1}H NMR: 3.00 (3H, s, CH_3), 2.30 (3H, s, *p*-CH_3), 7.10–8.40 (10H, m, C_9H_6N, C_6H_4), 15.90 (1H, s, NH) ^{13}C NMR: 20.93 (CH_3), 26.89 (*p*-CH_3), 115.12, 122.63, 126.76, 126.90, 127.49, 128.07, 133.05, 133.37, 136.15, 140.70, 145.22, 152.86 (aryl-C), 198.33 (C=O)
3p	^{1}H NMR: 1.00 (3H, t, CH_3), 1.75 (2H, m, CH_2), 3.05 (2H, q, CH_2), 2.3 (3H, s, *p*-CH_3), 7.1–8.4 (10H, m, C_9H_6N, C_6H_4), 15.85 (1H, s, NH) ^{13}C NMR: N.A.[a]
6c	^{1}H NMR: 1.00 (3H, t, CH_3), 1.80 (2H, m, CH_2), 2.90 (3H, s, N–CH_3), 3.10 (2H, q, CH_2), 7.10–8.40 (11H, m, C_9H_6N, C_6H_5) ^{13}C NMR: 12.17 (CH_3), 18.45 (CH_2), 39.63 (*N*–CH_3) 117.15, 123.02, 124.02, 127.04, 127.67, 129.05, 129.51, 129.75, 134.24, 138.24, 147.11, 148.35 152.09 (aryl-C), 200.95 (C=O)
6m	^{1}H NMR: 1.20 (3H, t, CH_3), 2.30 (3H, s, *p*-CH_3), 2.92 (3H, s, N–CH_3), 3.10 (2H, q, CH_2), 7.00–8.40 (10H, m, C_9H_6N, C_6H_4) ^{13}C NMR: 9.25 (CH_3), 20.01 (CH_2), 31.18 (CH_3), 34.57 (*N*–CH_3) 117.73, 124.48, 127.38, 128.04, 129.05, 129.94, 135.34, 135.31, 147.72, 148.35 155.19 (aryl-C), 200.65 (C=O)

[a] No satisfactory ^{13}C NMR spectra could be obtained for **3h** and **3p** compounds due to their low solubility in the NMR solvent $CDCl_3$.

which the –OH group is located away from nitrogen atoms of both the azo and the quinoline groups and, thus, has no intramolecular HB (Scheme 5). Although this tautomeric form is not stable and thus does not contribute to the tautomerization equilibria, it acts as a reference for the accuracy of the theoretical comparative results throughout this theoretical analysis.

As can be seen from the two trends, for both compounds, **C** is the next least stable tautomer. In addition to the lack of HB, the π-conjugation system in this tautomer is disconnected at the site of the α-carbon. It is thus expected that tautomer **C** will have the lowest stability, even lower than **G**. However, the stability of the ketone form of the local keto–enol

Table 3
IR and UV spectral data (in cm^{-1} and nm, respectively) obtained for the α-azo-2-ketomethylquinolines and *N*-methyl-α-azo-2-ketomethylquinolines introduced in Schemes 3 and 4, and Table 1

Entry	IR (neat)			UV (methanol)		
	C═O/C═C	C═C/C═O	N═N	λ_{max1}	λ_{max2}	λ_{max3}
3a	1660	1590	1510	398	307	247
3b	1665	1560	1515	399	305	246
3c	1665	1600	1540	399	302	246
3d	1600	1590	1520	399	302	246
3e	1660	1600	1520	400	306	245
3f	1660	1590	1510	402	325	242
3g	1675	1590	1510	412	322	244
3h	1675	1600	1510	414	329	244
3i	1680	1520	1500	415	327	243
3j	1645	1590	1510	402	335	241
3k	1640	1600	1515	415	335	241
3l	1640	1590	1520	404	330	244
3m	1665	1600	1515	406	330	248
3n	1660	1600	1510	419	328	241
3o	1660	1600	1530	406	304	247
3p	1660	1520	1500	407	328	244
6c	1665	1605	1510	405	305	245
6m	1660	1600	1515	405	327	248

tautomerism has compensated the instability resulting from the shortened conjugation system. The higher stability of the **D** tautomer compared to the **C** tautomer can be justified considering longer length of the conjugation system and possibility of forming intra-molecular HB in **D**, even though both have the same aromatic system. Steric hindrance between the methyl and quinoline hydrogen atoms does not allow strong intra-molecular HB within the co-planar structure of the **E** tautomer; the −C═O, and the ═N−N−H groups cannot be co-planar. In **3g**, the increased tendency for HB formation between the −C═O and the ═N−N−H groups, induced by the *p*-NO_2 substitution, is so strong that it imparts distortion to the co-planar structure with two independent aromatic groups tilted out of the HB plane. The strong HB thus compensates for the disconnection of the two π-systems and determines the binding energy of the most stable **E** tautomer for compound **3g**. Note that these results correspond to the isolated gas phase species (i.e. in the absence of any solvent and aggregation).

A comparison of the stability trends of the two compounds **3a** and **3g** shows that the NO_2 substitution at the X position

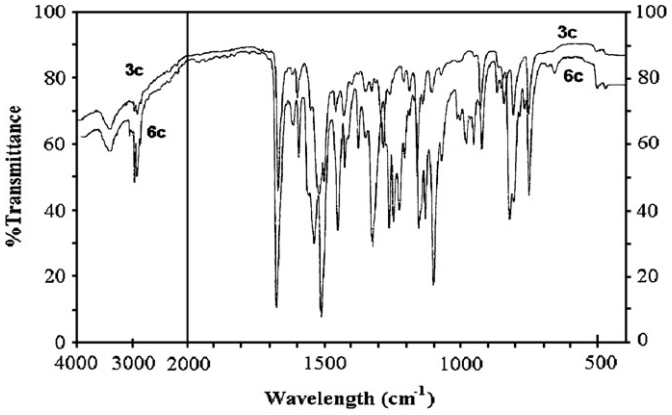

Fig. 1. Typical IR (in KBr disc) spectra of the enaminones (**3c** and **6c**) studied in this work.

significantly stabilizes **E** compared to all other tautomers and, at the same time, reduces the stability of the **F** tautomer. Both effects can be attributed to the fact that tautomer **E** has the closest exchange proton to the substituted $-NO_2$ group and, therefore, has the largest induced positive charge on this proton prior to HB formation; this results in a stronger HB involving this proton. It is obvious that the asymmetric HB (such as that exists in **E**) is much more sensitive to the changes in the bridging hydrogen than a symmetric HB (as is formed in **D**). Therefore, stabilization of the **E** tautomer is greater than that expected for the **D** tautomer upon introducing the *p*-NO_2 substituent on the phenyl ring. Induction of the *p*-NO_2 substitution in the **F** tautomer acts on the quinoline nitrogen atom electrons much more effectively than that on the enol oxygen atom electrons, and does makes the former less basic. This results in a weaker HB bond in **F** and makes it less stable.

The comparatively untouched positions of the **C** and **G** tautomers in the stability order can easily be understood if considering the non-HB hydrogen of **C** and the isolated (and thus non-HB) hydrogen of the **G** tautomer both of which remain almost intact upon the introduction of the *p*-NO_2 substituent. The effect of the $-NO_2$ group on the tautomers **A** and **B** is very small because of their farthest HB hydrogen atoms from this substitution.

Quantitatively, different effects would be expected for *o*-NO_2 and *m*-NO_2 substitutions on the same phenyl ring.

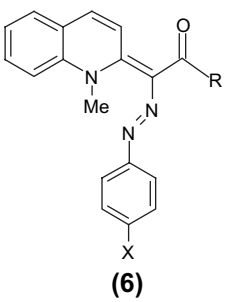

Scheme 4.

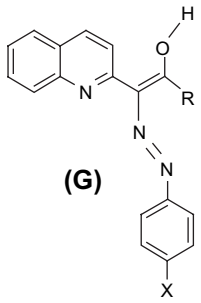

Scheme 5.

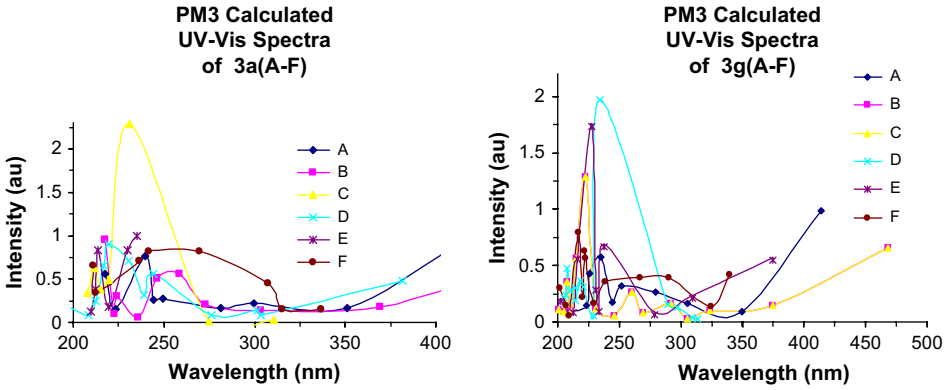

Fig. 2. PM3 calculated UV–vis spectra of **3a**(**A**–**F**) and **3g**(**A**–**F**).

In polar and especially protic solvents with HB capability, the preferred structures of these tautomers may be totally changed and therefore, the two trends obtained for stabilities of the two representative compounds may not be exactly followed. The actual comparative stabilities can be obtained via SCRF computations in which solvent effect is taken into account implicitly by different solvent–solute interaction models; such a demanding computation is beyond the scope and computer hardware facilities of the present work. However, solvent effects on the stability of the solute molecules can be studied indirectly by inspection of the electric dipole moments and atomic charges, as well as capability of forming one or two-way HB. A larger dipole moment results in stronger stabilizing interactions with the polar solvent molecules as bulk, and similarly, larger electric charges on the exposed atoms results in stronger local interactions with solvent molecules as individuals.

The calculated dipole moments show the following trends for the tautomers of the two compounds.

Dipole moment :

$$\mathbf{B} > \mathbf{C} > \mathbf{A} > \mathbf{D} > \mathbf{E} > \mathbf{G} > \mathbf{F} \quad (\mathbf{3a}: \mathrm{R} = \mathrm{CH_3},\ \mathrm{X} = \mathrm{H})$$

$$\mathbf{B} > \mathbf{A} > \mathbf{E} > \mathbf{G} > \mathbf{D} > \mathbf{F} > \mathbf{C} \quad (\mathbf{3g}: \mathrm{R} = \mathrm{CH_3},\ \mathrm{X} = \mathrm{NO_2})$$

The comparative analysis summarized in these trends shows that tautomer **B** has the largest bulk electrostatic interaction with polar solvents. Furthermore, the differences between the electric dipole moments of **A** and the next tautomer of the series are so significant that in polar solvents, **A** can be regarded to be more stable than all other tautomers having smaller dipole moments. This is while the larger dipole moment obtained for **C** cannot overcome the difference in their binding energies and thus cannot be accounted for any higher stability in the polar solvent. It can therefore be predicted that tautomers **A** and **B** are the most stable tautomers in polar solvents.

In protic solvents, all tautomers can form HB via their single exchangeable hydrogen and their basic centers (non-bonding electrons of the N and O atoms). The hydrogen atom engaged in HB is not readily accessible to the solvent molecules unless destroying the intra-molecular HB structure. Therefore, for protic and highly polar solvents with small molecules, it can be predicted that all protic tautomers (i.e. **C** is an exception) undergo severe conformational changes which can consequently alter the given gas phase PM3 stability orders and their relative statistical populations.

For the case of compound **3a** (with X = H), it seems that charges on and the separation between the oxygen atom (as the most negative center) and the exchanging hydrogen atom (as the most positive center) determines the size and direction of the dipole moment vector. Since these two atoms have the smallest separation in **F** and **G**, these two tautomers have the smallest dipole moments, and thus the least initial interaction (prior to any conformational changes induced by the solvent molecules to achieve thermodynamically more stable states) with polar solvents. For compound **3g** (with $X = NO_2$), in addition to the separation between these two oxygen and hydrogen atoms, their relative positions with respect to the position of the NO_2 group also play important role, because its oxygen atoms (as negative centers) together with the positive exchanging hydrogen atom form considerably larger local dipole moments. The two local component dipole moments may thus result in an increased or a decreased overall (resultant) dipole moment. Compared to all tautomers of **3a**, size of the dipole moment is significantly larger in the corresponding tautomers

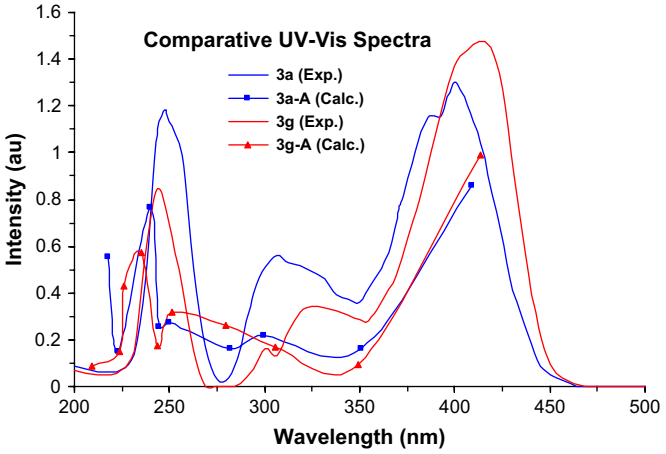

Fig. 3. Comparison of experimental UV–vis spectra of **3a** and **3g** with the PM3 calculated spectra of **3a**-**A** and **3g**-**A**.

Table 4
Numerical values of the PM3 calculated quantities and parameters of all tautomers of compounds **3a** and **3g**

Tautomer	Compound **3a**					Compound **3g**				
	$\|E_b\|$	μ	E_{HOMO}	E_{LUMO}	E_{ex} (dipole)	$\|E_b\|$	M	E_{HOMO}	E_{LUMO}	E_{ex} (dipole)
A	4182.0	3.800	−8.041	−1.205	653 (1.16)	4371.6	9.032	−8.425	−1.628	634 (8.34)
B	4181.0	5.133	−8.042	−1.219	705 (5.16)	4370.3	10.256	−8.446	−1.740	797 (8.92)
C	4179.1	4.220	−9.301	−0.790	472 (4.39)	4368.7	5.665	−9.522	−1.717	538 (9.11)
D	4181.7	2.645	−8.457	−1.082	499 (6.27)	4371.4	6.901	9–9.02	6–1.54	6469 (5.5)
E	4180.5	2.204	−8.616	−0.868	420 (1.93)	4372.1	8.090	−9.3815	−1.131	437 (7.78)
F	4182.4	1.510	−8.572	−0.876	473 (3.31)	4371.3	6.467	−8.935	−1.492	582 (8.20)
G	4171.2	1.737	−8.519	−0.755	476 (1.32)	4364.4	7.344	−9.207	−1.424	555 (9.83)

Binding energy $|E_b|$ are given in kcal/mol, dipole moment μ in Debye, resistance to oxidation in terms of HOMO energy E_{HOMO} in eV, electron capture potential in terms of LUMO energy E_{LUMO} in eV, and non-optical CI excitation energy E_{ex} in nm (and the excited state dipole moment in Debye).

of **3g**. Exceptional behavior (displaced position) of the **C** tautomer of **3g** is due to the fact that the two component dipole moments mentioned above cancel each other effectively as opposed to the cooperative addition happening in other tautomers.

Analysis of the atomic charges on the electronegative elements in the PM3 optimized structures shows that strength of local electrostatic interactions and the basic centers (O and N atoms) HBs with the polar solvents having small molecules and the protic solvents have the following orders.

Atomic charges :

$$\mathbf{A} > \mathbf{B} > \mathbf{E} > \mathbf{D} > \mathbf{F} > \mathbf{C} > \mathbf{G} \quad (\mathbf{3a}: \mathrm{R} = \mathrm{CH_3},\ \mathrm{X} = \mathrm{H})$$

$$\mathbf{A} > \mathbf{B} > \mathbf{D} > \mathbf{F} > \mathbf{C} \cong \mathbf{E} > \mathbf{G} \quad (\mathbf{3g}: \mathrm{R} = \mathrm{CH_3},\ \mathrm{X} = \mathrm{NO_2})$$

As can be seen from these trends, tautomers **A** and **B** of both compounds are very similar in their local charge interactions (via the exposed electronegative atoms) with molecules of polar solvents. Since dipole moment vectors of the **A** and **B** tautomers of both compounds show a reverse trend, are larger than those of the corresponding **A** tautomers, it can be concluded that the overall polar solvent effects on these two tautomers are identical. Therefore, the comparative stability trends found for these two tautomers are valid also in polar solvents. The two trends show also that compared to other tautomers, **A** and **B** are engaged in much more stronger stabilizing local interactions with polar solvent molecules in addition to their strongest bulk interactions inferred from dipole moments. Therefore, it can safely be predicted that **A** and **B** are the dominant tautomers in polar solvents.

The opposite orders of the PM3 atomic charges and dipole moments found for the couple **D** and **E**, predict overall similar solvent effects on the structural and electronic characteristics of these two tautomers. It can thus be predicted that the comparative thermodynamic stabilities of tautomers **D** and **E** in polar solvents be the same as that we obtained for the gas phase species. Note that the atomic charges define the short range and local interactions and HB capability, while dipole moments determine the global interactions with solvent. Both sets of interactions contribute to the solvent stabilization or destabilization of the solute molecules.

The calculated vibrational spectra, while clearly differentiating between the tautomers, cannot be used to predict relative susceptibility of these tautomers to the environmental (thermal) degradation via environmental radiations in the range of IR and longer wavelengths.

No satisfactory correspondence could be established between the PM3 calculated and experimental IR and UV–vis spectra. This failure could be attributed to the large contributions from gas-to-liquid shifts and intermolecular interactions (both solvent–solute and solute–solute) to both wavelength and intensity of the experimentally observed spectra [22–24]. Analysis of the calculated vibrational spectra suggests that the –OH band in the IR spectra would be a useful characteristic to differentiate among possible tautomers. Practically, it is always a difficult task to avoid water vapor and impurity in the experimental setup.

In spite of the fact that the numerical values of the peak positions in the calculated UV–vis spectra (Fig. 2) do not correspond to the experimental results, the structures of the calculated spectra of **3a**-**A** and **3g**-**A** are almost identical to the respective experimentally observed spectra of **3a** and **3g** compounds (Fig. 3). The interesting point is that the experimental spectra of both compounds (actually all **3a**–**p** compounds) have very similar structures. This similarity suggests that these two compounds adopt one single tautomeric form dominantly. Furthermore, the PM3 computational results presented in Figs. 2 and 3 confirm that this single tautomeric form is **A**.

The numerical values of the quantities analyzed in this theoretical study are provided in the supplementary data.

A kinetic study [25] could also be carried out on the tautomerization rates, provided the experimental data could have been obtained. The numerical values of the quantities analyzed in this theoretical study are provided in Table 4.

Appendix. Supplementary data

Supplementary data associated with this article can be found, in the online version, at doi:10.1016/j.dyepig.2006.10.003.

References

[1] Greenhill JV. Chem Soc Rev 1977;6:277.
[2] Gawinecki R, Osmialowski B, Kolehmainen E, Nissinen M. J Mol Struct 2000;525:233.

[3] Greenhill JV, Loghmani-Khouzani H, Maitland DJ. Tetrahedron 1988;44:3319.
[4] Greenhill JV, Loghmani-Khouzani H, Maitland DJ. J Chem Soc Perkin Trans 1 1991;2831.
[5] Douglass JE, Elba M, Ataei A, Dotson DL, Lo HH. J Heterocycl Chem 1992;29:1361.
[6] Kolehmainen E, Osmialowski B, Krygowski TM, Kauppinen R, Nissinen M, Gawinecki R. J Chem Soc Perkin Trans 2 2000;1259.
[7] Eistert VB, Enders E. Liebigs Ann Chem 1970;734:56.
[8] Yamazaki M, Noda K, Hamana H. Chem Pharm Bull 1970;18:901.
[9] Kawase M, Teshima M, Saito S, Tani S. Heterocycles 1988;48:2103.
[10] Mondelli R, Merlini L. Tetrahedron 1966;22:3253.
[11] Katritzky AR, Ghiviriga I, Oniciu DV, O'Ferrall RA, Walsh SM. J Chem Soc Perkin Trans 2 1997;2605.
[12] Cheon KS, Park YS, Kazmaier PM, Bunncel E. Dyes Pigments 2002;53:3.
[13] Garnovski AD, Uraev AI, Minkin VI. Arkivoc 2004;29.
[14] Alt GH. J Org Chem 1966;31:2384.
[15] Bail P, Nicholls CH. Dyes Pigments 1982;3:5.
[16] Lycka A, Vrba Z, Vrba M. Dyes Pigments 2000;47:45.
[17] Tait KM, Parkinson JA, Jones AC, Ebenezer WJ, Bates SP. Chem Phys Lett 2003;374:372.
[18] Lycka A. Dyes Pigments 1999;43:27.
[19] Greenhill JV, Loghmani-Khouzani H. Spectrochim Acta 1990;46A: 803.
[20] Stewart JJP. Comput J Chem 1989;10:209;
Stewart JJP. Comput J Chem 1989;10:221;
Stewart JJP. Comput J Chem 1991;12:320.
[21] HyperChem, release 7.0 for Windows, molecular modeling system. HyperCube, <http://www.hyper.com>; 2002.
[22] Jensen F. Introduction to computational chemistry. Chichester: Wiley VCH; 1999.
[23] Levine IL. Quantum chemistry. 5th ed. New Jersey: Prentice-Hall; 2000.
[24] Foresman JB, Head-Gordon M, Pople JA, Frisch M. J Phys Chem 1992;96:135.
[25] Tauro S, Coutinho E. J Mol Struct (Theochem) 2000;532:23.